Journal of Supramolecular Structure 2:609–616 (1974)

LIPID PHASE SEPARATIONS AND PROTEIN DISTRIBUTION IN MEMBRANES

W. Kleemann, C. W. M. Grant, and H. M. McConnell

Stauffer Laboratory for Physical Chemistry, Stanford, California 94305

Lateral phase separations in lipid and lipid-protein systems are discussed with the aid of phase diagrams derived from spin-label measurements. Freeze-fracture data from E. coli membranes and model lipid–protein bilayers indicate that the protein tends to associate with fluid lipid phases.

Phospholipid suspensions in excess water often form multibilayers. The lipid molecules can assume a low temperature array (gel phase) in which their acyl chains are rigidly extended, or at higher temperatures they can undergo a concerted transition to a state of greater flexibility (fluid or liquid–crystalline phase). Thermally induced fluid-gel transitions in bilayers formed from mixtures of several different lipids can be described by phase diagrams. This approach was first used by Phillips et al. (1) and was later systematically developed by Shimshick and McConnell (2, 3). We shall review some work which has been going on in our laboratory since the 1973 Squaw Valley conference at which earlier work was summarized (4). The phenomena described are considered only briefly here since more elaborate discussions and data are or will be presented in detailed publications.

For pure lipids the fluid-gel transition occurs at a well-defined temperature which can be measured spectroscopically using the spin label, TEMPO (2, 2, 6, 6-tetramethyl-piperidine-1-oxyl) (1). TEMPO dissolves readily in water and in fluid hydrocarbon regions of lipid bilayers (5) but is largely excluded from solid or gel phase regions. In the presence of hydrated lipids, TEMPO partitions between aqueous and fluid lipid regions. Since the hyperfine and g-tensors of the EPR spectrum depend on the polarity of the spin-label environment, the high field spectral line can be resolved into signals from the aqueous and lipid regions of the sample. This permits one to measure a TEMPO spectral parameter, f, which is approximately equal to the fraction of TEMPO dissolved in the (fluid) lipid phase of the sample. It will be convenient here to refer to the gel or solid phase as S and the fluid phase as F. At low temperatures, where only S phase is present, the value of f is small. At high temperatures, i.e., above the transition temperature, T_t, the value of f is large since TEMPO is quite soluble in F state lipids. A schematic plot of f vs. 1/T for a

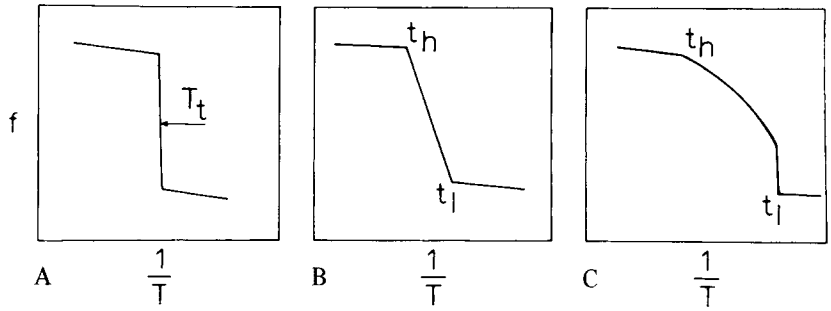

Fig. 1. Schematic plots of the TEMPO spectral parameter f as a function of 1/T for (A) a pure lipid, (B) a binary lipid mixture forming a solid solution, and (C) a binary lipid mixture with partial solid phase immiscibility.

pure phospholipid is shown in Fig. 1A. Shimshick and McConnell have used this technique to measure T_t for a number of phospholipids (2).

Freeze-fracture electron microscopy can sometimes be a useful technique for studying the fluid-gel behavior of lipid bilayers. For instance the freeze-fracture appearance of DML* and a number of other phosphatidylcholines is different depending upon whether the samples are quenched from above or below T_t (6–9). A freeze-fracture electron micrograph of a DML vesicle cryogenically fixed from below T_t is presented in Fig. 2A. Note the regular pattern of lines on the lipid. No such regular patterns are seen when the same sample is quenched from above T_t. Instead the lipid is smooth or displays a jumbled pattern (Fig. 2B). The jumbled pattern shown in Fig. 2B results when the cryogenic fixation rate of fluid lipid is not fast enough (7, 9) so that upon passing through T_t the lipid molecules have a limited time to begin to reorganize to their S phase. This partial failure to preserve F phase morphology by cryogenic fixation in no way prevents distinction between F and S phase lipid and can in fact be a very useful phenomenon.

Unlike a pure lipid, a binary lipid mixture dispersed in water does not display a sharp transition temperature. Rather, *two* characteristic temperatures are found, t_h and t_l. Above t_h, the higher characteristic temperature, all the lipids are in the F state; below t_l all the lipids are in the S state. Between t_h and t_l domains of S phase and F phase are simultaneously present in the bilayer. In the plot of f vs. 1/T gradual decrease of f is observed between t_h and t_l instead of the precipitous drop at T_t for a pure lipid. This is shown schematically in Fig. 1B. The best way to graph the behavior of such a binary system as a function of composition and temperature is with a phase diagram such as those shown schematically in Fig. 3. Above the fluidus curve in Fig. 3 all the lipid is in the fluid state; thus t_h defines the points on the fluidus curve. Similarly, t_l defines the solidus curve. The region between the fluidus and the solidus is the region of coexistence of F and S phase. The binary lipid systems studied by Shimshick and McConnell approach two general types of phase diagram. One is the solid solution–fluid solution case shown in Fig. 3A. Over the

*Abbreviations: DML, dimyristoyllecithin; DPL, dipalmitoyllecithin; DSL, distearoyllecithin; DEL, dielaidoyllecithin; DPPE, dipalmitoylphosphatidylethanolamine.

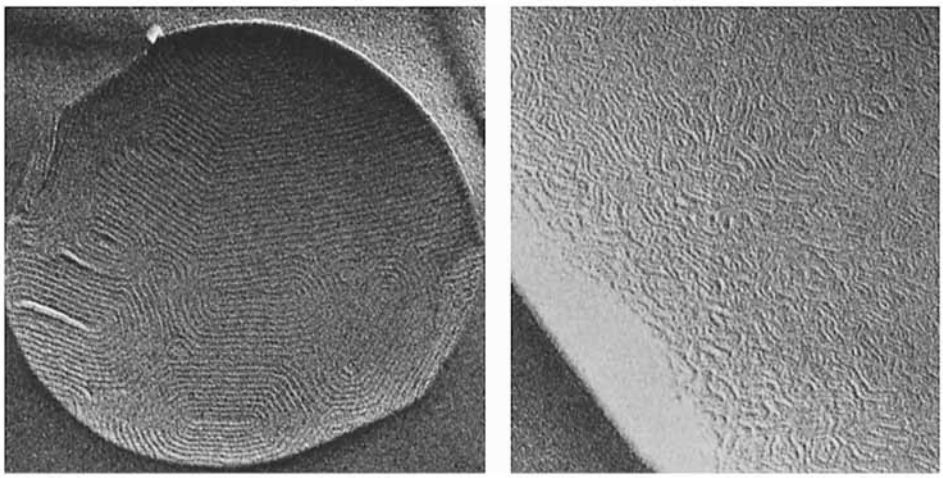

A B

Fig. 2. Freeze-fracture micrographs of DML vesicles prepared by dialysis of a lipid–detergent mixture. The samples were quenched from (A) 14.5° and (B) 37°. T_t for DML is 23°. (× 60,000)

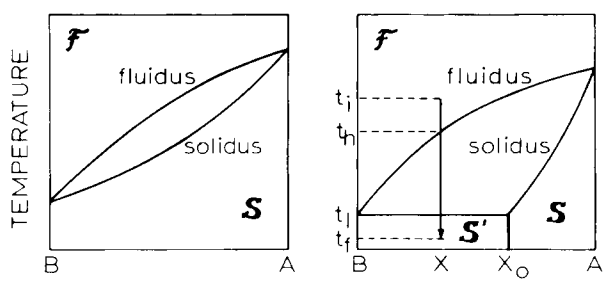

A B

Fig. 3. Schematic phase diagrams for binary lipid mixtures (A) forming a solid solution and (B) exhibiting partial solid phase immiscibility.

whole range of compositions the solid is miscible. This occurs when the two lipids are quite similar in nature, for instance, DML–DPL or DPL–DSL (2). The other type is shown in Fig. 3B and is found when the lipids are more different in their physical characteristics, i.e., DML–DSL, DML–DPPE, DPL–DPPE, DML–cholesterol and DPL–cholesterol (3, 4). In these cases the lipids exhibit only partial miscibility in the solid phase and over a certain range of compositions two solid phases coexist as a thermodynamically determined heterogeneous mixture. If a mixture of composition X (Fig. 3B) is slowly cooled from an initial temperature, t_i, to a final temperature, t_f, some solid starts to form when t_h is reached. This appears as the breakpoint at t_h in Fig. 1C. More and more solid forms as the temperature is lowered further, until a little above t_l the solid phase has a composition almost equal to X_0 and the fluid phase is almost pure B. A further lowering

TABLE I. Predictions from the Phase Diagram DEL–DPL

DEL/DPL	Temperature	Phases
50/50	36°	All fluid*
50/50	30°	Both, more fluid
50/50	25°	About equal amounts fluid and solid**
50/50	17°	Both, more solid
50/50	10°	All solid
25/75	15°	All solid

*Fluid here stands for the high temperature form of the lipid; generally referred to as liquid-crystalline or F phase.

**Solid stands for the low temperature form of the lipid, usually called gel or S phase.

of the temperature leads to the sudden freezing of *all* the remaining fluid lipid. This event shows up as a precipitous drop in f on the f vs. 1/T diagram in Fig. 1C. It should be emphasized that in the S′ phase two different solids are present at equilibrium.

Both types of phase diagram predict solid and fluid phases to coexist between the fluidus and the solidus curves. These phases form patches in the bilayers which are large enough to actually be observed in freeze-fracture preparations (4, 8). Thus Grant et al. (10) checked the predictions of the spin-label-derived phase diagram for mixtures of DEL and DPL. These are listed in Table I. In all cases the predictions were verified, i.e., for "fluid" the lipid regions appeared jumbled and for "solid" regular line patterns were observed. It should be noted that at 36° only fluid lipids are found, although T_t for DPL is 41°, and that for 75% DPL only solid is observed at 15°, which is above the T_t of 12° for DEL (10). Thus the freeze-fracture experiments provide dramatic support for the correctness and predictive power of the phase diagrams obtained by EPR measurements.

Biological membranes have a more complex lipid composition and also contain proteinacious material in the bilayer. Nevertheless, there will always be characteristic temperatures related to t_h and t_l which border an intermediate region of lateral phase separation phenomena arising from lipid-lipid interactions. It has been possible to measure these temperatures for the inner membranes of an Escherichia coli mutant (11). This mutant is an unsaturated fatty acid auxotroph and is also deficient in β-oxidation. Thus it can only incorporate those unsaturated fatty acids supplied in the medium and cannot alter them. When grown on elaidic acid the composition of the membrane lipids is especially simple (12). It approximates a binary system with 70% dielaidoyl phosphatidylethanolamine and 30% elaidoyl palmitoyl (or myristoyl) phosphatidylethanolamine. Measurements of the TEMPO parameter give the values of 38° for t_h and 31° for t_l. The lipid extracts from these membranes show similar characteristic temperatures to those found in the membranes and so the temperatures must be largely determined by the bulk lipid. Freeze-fracture electron microscopy shows that the appearance of the plasma membrane of whole cells differs, depending on whether the sample was quenched from above or below t_h (13). Similar observations have been made by others on Acholeplasma laidlawii (7, 14, 15), yeast cells (16), and Tetrahymena (17, 18). The results for the E. coli are summarized in Table II. Clearly, the interpretation is not as straightforward as in the case of model bilayers. Above t_h the distribution of

TABLE II. Freeze-Fracture Appearance of the Plasma Membrane of the E. coli Mutant Grown on Elaidic Acid

Temperature	Particle Distribution	
	No Fixation	Fixed with Glutaraldehyde
Above t_h	Netlike*	Random**
Between t_h and t_l	Aggregated†	Aggregated
Below t_l	Aggregated	Aggregated

*The particles, presumably protein-related, are distributed in a netlike arrangement, with small round patches (50–100 nm diameter) void of particles.

**No special order to the particle distribution, all areas of the plasma membrane are covered equally.

†Particles are aggregated into large patches, leaving other large membrane areas void of particles.

particles in the unfrozen membrane is probably random. We feel that the round patches void of particles in the case of unfixed cells quenched from above t_h are a reflection of the fact that the cryogenic fixation rate is not infinitely fast. Between t_h and t_l solid and fluid lipid regions should be present simultaneously. If the protein prefers a fluid lipid environment, it can be expected to concentrate in fluid domains. Unfortunately, in this case the solid lipids do not form regular line patterns and it is not possible to positively identify fluid and solid regions from the freeze-fracture micrographs.

Below t_l there should be either a solid solution of the lipids or a coexistence of two different solid phases, depending on which phase diagram applies to this membrane system. The aggregation of particles seen would point to the second possibility, but the other possibility cannot be excluded. The aggregation could be due to retention of the phase separation below t_l because equilibrium cannot be attained as a result of slow kinetics, i.e., a random equilibrium distribution is prevented by too slow lateral diffusion. The TEMPO parameter plot actually looks more like that for a system which forms a solid solution of the lipids (Fig. 1B). When a fluid lipid sample is quenched by the normal method there is a brief period during which the lipid can respond to the dropping temperature before being literally frozen in place. The small round patches void of particles that form if an unfixed cell is quenched from above t_h could be due to a beginning phase separation of the lipids in which the protein molecules follow the fluid phase. A similar effect, in which a relatively fast cooling process leads to a nonequilibrium distribution and "round patch" appearance in the solid, is known as "coring" in metal alloys (19). Alternatively, the lipid system could freeze as a pseudo single lipid component and bring about a partial protein–lipid phase separation.

Much of the difficulty in interpreting these observations arises from the fact that the complete phase diagram of the lipids is not known. It is therefore advantageous to study a binary lipid system with known phase diagram and to incorporate protein molecules into the bilayer. The distribution of particles as a function of quenching temperature can then be readily investigated.

We have studied 50/50 mole % mixtures of DEL/DPL and DML/DSL containing glycophorin (20), the major glycoprotein of human red blood cells. The pure glycoprotein (21) can be reincorporated by a technique analogous to that used by Hong and Hubbell

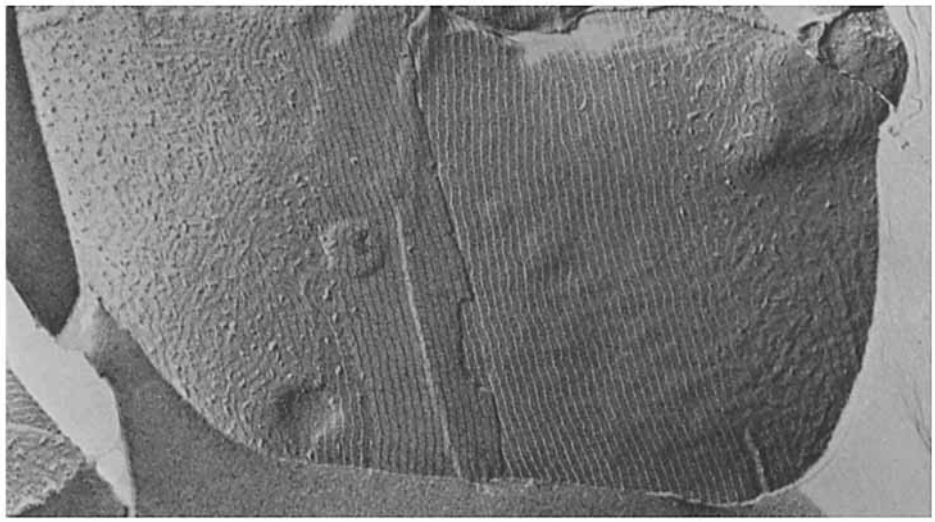

Fig. 4. A 50/50 mole % mixture of DEL/DPL into which glycophorin was incorporated by dialysis. The samples were quenched from 23°, which is between the fluidus and solidus curves. (× 80,000)

(22) to generate lipid bilayers containing rhodopsin. Freeze-fracture electron micrographs of lipid bilayers containing glycophorin display particles in their fracture faces somewhat smaller than those seen in erythrocytes. Patterns in the lipids themselves demarcate F and S phase domains as mentioned earlier. Above t_h the particles are randomly distributed. Below t_h but above t_l the lipid separates into S and F phase regions as predicted by the phase diagrams. The glycoprotein-related particles are associated almost exclusively with fluid domains at equilibrium (Fig. 4). In pure phospholipids such as DML and DPL, glycophorin is randomly dispersed in the bilayers both above and below T_t. These results show that, in the case of glycophorin, the protein–lipid interfacial free energy is minimized in the presence of F phase lipid, but that the glycoprotein is by no means rigorously excluded from S phase lipid.

A more dramatic preference for F phase lipid bilayers has been observed in the case of the $(Mg^{2+} + Ca^{2+})$ ATPase from rabbit sarcoplasmic reticulum (Kleemann and McConnell, unpublished observations). The ATPase was purified by the method of Warren et al. (23) and incorporated into DML vesicles by the dialysis technique of Racker (24). In Fig. 5 the freeze-fracture appearance of this preparation is shown. In samples quenched from above T_t (Fig. 5A), the ATPase-related particles are randomly distributed on the lipid fracture face which also displays jumbled lines characteristic of F phase lipid. When the vesicle preparation is cooled through T_t prior to quenching, the particles are excluded from growing S phase lipid regions and are often pushed into lines or patches (Fig. 5B). Chen and Hubbell (25) have observed that bleached rhodopsin is randomly distributed in pure DML but that unbleached rhodopsin is excluded from the solid phase as the lipid freezes. Thus it seems that the ATPase in DML vesicles has a distribution similar to that of dark-adapted rhodopsin whereas glycophorin behaves like bleached rhodopsin. Presumably bleaching rhodopsin induces a protein conformation change such that the lipid–protein

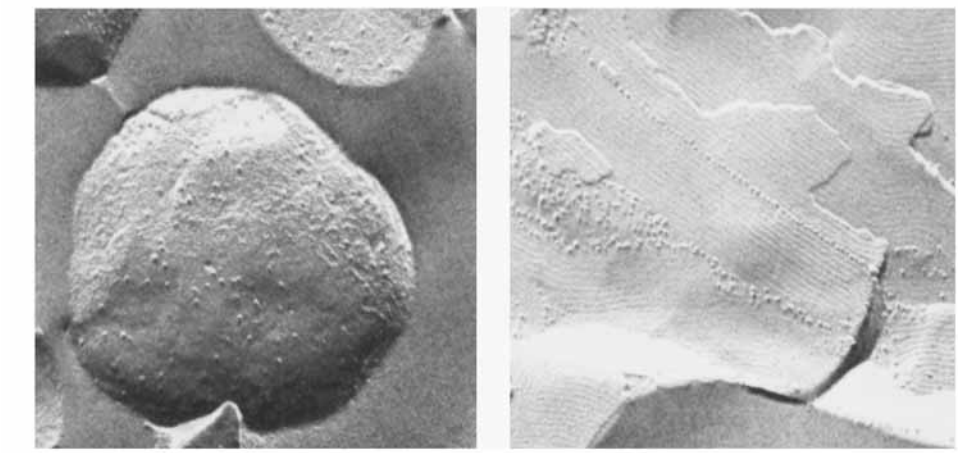

Fig. 5. DML vesicles with ATPase incorporated into the bilayer by dialysis. The samples were quenched from (A) 30° and (B) 17°. (× 80,000)

interactions are altered from ATPase-like to glycophorin-like.

It may well be that this preference for F phase lipid bilayers is a property common to many proteins. Such a phenomenon readily explains the previously mentioned freeze-fracture observations on inner membranes of the E. coli mutant grown on elaidic acid. It is likely that in the red blood cell a protein network of spectrin holds glycophorin in a dispersed array (26). Our work suggests that certain more fluid lipids will tend to form pools or clusters associated with the glycoprotein. It is interesting to speculate that if the spectrin system has actomyosin-like contractile properties (26) the erythrocyte would possess a system which could potentially modify not only protein and lipid distribution but also lipid fluidity in response to hormonal (or other) stimuli (27, 28).

ACKNOWLEDGMENTS

C. W. M. Grant was a NRC of Canada NATO postdoctoral fellow from 1972–1974. This work was supported by NSF Grant No. 33501X2. It has benefited from facilities made available to Stanford University by the Advanced Research Projects Agency through the Center for Materials Research.

REFERENCES

1. Phillips, M. C., Ladbrooke, B. D., and Chapman, D., Biochim. Biophys. Acta 196:35 (1970).
2. Shimshick, E. J., and McConnell, H. M., Biochem. 12:2531 (1973).
3. Shimshick, E. J., and McConnell, H. M., Biochem. Biophys. Res. Comm. 53:446 (1973).
4. Shimshick, E. J., Kleemann, W., Hubbell, W. L., and McConnell, H. M., J. Supramol. Struct. 1:285 (1973).

5. Hubbell, W. L., and McConnell, H. M., Proc. Nat. Acad. Sci. 61:12 (1968).
6. Pinto da Silva, P., J. Microscopie 12:185 (1971).
7. Verkleij, A. J., Ververgaert, P. H. J., van Deenen, L. L. M., and Elbers, P. F., Biochim. Biophys. Acta 288:326 (1972).
8. Ververgaert, P. H. J. Th., Verkleij, A. J., Elbers, P. F., and van Deenen, L. L. M., Biochim. Biophys. Acta 311:320 (1973).
9. Ververgaert, P. H. J. Th., Verkleij, A. J., Verhoeven, J. J., and Elbers, P. F., Biochim. Biophys. Acta 311:651 (1973).
10. Grant, C. W. M., Wu, S. H. W., and McConnell, H. M., Biochim. Biophys. Acta 363:151 (1974).
11. Linden, C. D., Wright, K. L., McConnell, H. M., and Fox, C. F., Proc. Nat. Acad. Sci. 70:2271 (1973).
12. Linden, C. D., Keith, A. D., and Fox, C. F., J. Supramol. Struct. 1:523 (1973).
13. Kleemann, W., and McConnell, H. M., Biochim. Biophys. Acta 345:220 (1974).
14. Branton, D., Elsgaeter, A., and James, R., in "Mitochondria and Biomembranes," (Proc. of the 8th meeting of FEBS), p. 165 North-Holland Publishing Co., Amsterdam (1972).
15. James, R., and Branton, D., Biochim. Biophys. Acta 323:495 (1973).
16. James, R., Branton, D., Wisnieski, B., and Keith, A., J. Supramol. Struct. 1:38 (1972).
17. Speth, V., and Wunderlich, F., Biochim. Biophys. Acta 291:621 (1973).
18. Wunderlich, F., Speth, V., Batz, W., and Kleinig, H., Biochim. Biophys. Acta 298:39 (1973).
19. Rhines, F. N., "Phase Diagrams in Metallurgy," p. 24. McGraw-Hill, New York (1956).
20. Grant, C. W. M., and McConnell, H. M., Proc. Nat. Acad. Sci. (in press).
21. Jackson, R. L., Segrest, J. P., Kahane, I., and Marchesi, V. T., Biochemistry 12:3131 (1973).
22. Hong, K. and Hubbell, W. L., Biochemistry 12:4517 (1973).
23. Warren, G. B., Toon, P. A., Birdsall, N. J. M., Lee, A. G., and Metcalfe, J. C., Proc. Nat. Acad. Sci. 71:622 (1974).
24. Racker, E., J. Biol. Chem. 247:8198 (1972).
25. Chen, Y. S., and Hubbell, W. L., Exp. Eye Res. 17:517 (1973).
26. Juliano, R. L., Biochim. Biophys. Acta 300:341 (1973).
27. Kury, P. G., Ramwell, P. W., and McConnell, H. M., Biochem. Biophys. Res. Comm. 56:478 (1974).
28. Huestis, W. H., and McConnell, H. M., Biochem. Biophys. Res. Comm. 57:726 (1974).